J Mater Sci (2007) 42:10152–10159
DOI 10.1007/s10853-007-2099-3

Mixed conducting oxides $Y_xZr_{1-x-y}Ti_yO_{2-x/2}$ (YZT) and corresponding Ni/YZT cermets as anode materials in an SOFC

X. Mantzouris · N. Zouvelou · V. A. C. Haanappel · F. Tietz · P. Nikolopoulos

Received: 29 March 2007 / Accepted: 13 August 2007 / Published online: 25 September 2007

Abstract The physical properties of mixed-conducting oxides in the ternary system Y_2O_3–ZrO_2–TiO_2 with the general formula $Y_xZr_{1-x-y}Ti_yO_{2-x/2}$ (YZT, where $0.133 < x < 0.25$ and $0 < y < 0.15$) are presented and evaluated in terms of an application as anode materials in solid oxide fuel cells (SOFCs). The total electrical conductivity of the ceramics with cubic fluorite structure in air mainly depends on the Ti content and decreases at 900 °C by about one order of magnitude from $y = 0$ to $y = 0.15$. Comparing the conductivity of contributions at 900 °C in Ar/4% H_2 the highest contributions of electronic conductivity were obtained for $y = 0.15$. For the Ni/YZT cermets, the enhanced adherence at the metal/ceramic interface, compared to Ni/8YSZ (8 mol% yttria stabilised zirconia), results in a better long-term stability in terms of electrical conductivity and microstructure after 1,000 h of annealing at 1,000 °C in reducing atmosphere. The electrochemical performance, tested in fuel cells with Ni/8YSZ, Ni/$Y_{0.20}Zr_{0.75}Ti_{0.05}O_{1.9}$ and Ni/$Y_{0.20}Zr_{0.70}Ti_{0.10}O_{1.9}$ anodes, decreased for Ni/$Y_{0.20}Zr_{0.70}Ti_{0.10}O_{1.9}$ under steam reforming conditions, most likely due to the reduced ionic conductivity of this specific YZT ceramic.

X. Mantzouris · N. Zouvelou · P. Nikolopoulos
Department of Chemical Engineering, University of Patras, 26504 Patras, Greece

V. A. C. Haanappel · F. Tietz (✉)
Forschungszentrum Jülich GmbH, Institut für Energieforschung (IEF), 52425 Julich, Germany
e-mail: f.tietz@fz-juelich.de

Introduction

Cermet anodes with mixed-conducting ceramic phase are preferable materials regarding an extension of the electron transfer reaction zone for fuel gas conversion and minimisation of the nickel content of the anode to achieve a redox stable anode. Partial substitution in 8YSZ by titania is known to increase the electronic conductivity in reducing atmosphere [1–9].

As pure mixed-conducting ceramic anodes, however, there are concerns about the poor electronic conductivity of n-type conductors and their catalytic properties [10–12]. Therefore the use of Ni as a catalyst is indispensable to obtain high-performance anodes. A promising material combination as a cermet anode seems to be a mixed conducting oxide material such as zirconia containing yttria and titania in combination with Ni [13–16].

With respect to the application as an anode substrate, benefit of Ni/YZT cermets is the reduction of the sintering of Ni particles due to the improved interfacial bonding at the ceramic/metal interface [17, 18], compared to the "state-of-the-art" electrode Ni/8YSZ [18, 19].

In the present work, mixed-conducting oxides with the general formula $Y_xZr_{1-x-y}Ti_yO_{2-x/2}$ (YZT) are characterised and their electrical conductivity is examined in air and Ar/4%H_2 atmosphere with respect to their possible application as the ceramic component in the anode cermet material (Ni/YZT) of an SOFC. In addition, the stability of the cermets containing 30, 40 and 45 vol% Ni is investigated by measuring their electrical conductivity after long-term annealing at 1,000 °C in reducing atmosphere combined with microstructure analysis. Finally, on the basis of electrochemical tests carried out on fuel cells with Ni/YZT anodes, the influence of the titania content on the performance of Ni/YZT anodes is discussed.

Experimental procedure

Powder preparation

Various ceramic compositions were chosen for two different sets of materials: (a) the substitution of Zr by 5 and 10 at% Ti in 20 mol% $YO_{1.5}$ + 80 mol% ZrO_2 as well as 5 and 15 at% in 25 mol% $YO_{1.5}$ + 75 mol% ZrO_2 in the cubic phase field (series A, samples 1–4) and (b) admixture of 5 and 10 at% Ti in 8YSZ along the cubic–tetragonal (c–t) phase boundary [20, 21] of the ternary $YO_{1.5}$–ZrO_2–TiO_2 phase diagram shown in Fig. 1, as well as pure 8YSZ (series B, samples 5–7).

The compositions of series A were synthesised by homogeneous co-precipitation with a diluted ammonia solution using mixtures of nitric acid and the starting materials $Y(NO_3)_3 \cdot 5H_2O$, $ZrOCl_2 \cdot 8H_2O$ and $TiCl_3$ in HCl in the appropriate amounts [22]. The precipitates were washed until no chloride ions could be detected with a silver nitrate solution. The compositions of series B were synthesised by spray-drying of aqueous nitrate solutions using the corresponding metal nitrate precursors as described in detail elsewhere [23]. For the crystal structure formation all powders were calcined at 900 °C for 5 h in air.

Sample preparation

For the crystal structure investigations small amounts of the powders were sintered up to 1,400 °C for 5 h in air in steps of 100 °C and subjected to X-ray diffraction (XRD). The experiments were performed at room temperature using a Philips PW 1830/40 diffractometer and Cu K_α radiation.

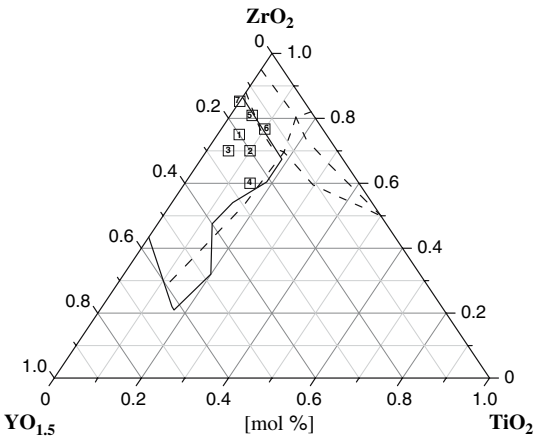

Fig. 1 The ternary phase diagram showing the Zr-rich phase regions [20] (dashed lines) and the single-phase cubic fluorite region [21] (solid line), as well as the positions of the tested powders

For the preparation of cermets, parts of the ceramic powders, sintered at 1,400 °C for 5 h in air, were mixed with the appropriate amounts of NiO (J. T. Baker, >99%) to achieve Ni contents of 30, 40 and 45 vol% after reduction. All powders and powder mixtures were wet-milled with ethanol in a centrifugal ball mill for 50 h in order to homogenise the mixture and reduce the mean grain size.

Electrical and electrochemical measurements

The electrical conductivity measurements were performed by the standard four-probe d.c. technique using rectangular bars (3 × 3 × 25 mm), which were uniaxially pressed and sintered at 1,400 °C for 5 h. The current and voltage were measured by calibrated multimeters (Keithley) and the appropriate software program (Test Point). The density of the samples after sintering was at least between 83 and 95% of the theoretical density. The specimens that contained NiO were sintered at 1,300 °C for 5 h and subsequently reduced in flowing Ar/4% H_2 atmosphere at 900 °C for 5 h. After the reduction of NiO the cermets had a porosity of 20–25%.

Four silver wires were wrapped around the sintered rectangular bars at four locations at symmetrically equal distances from the ends and intimate contact was achieved by using conducting silver paste (Demetron Leitsilber 200). In order to resolve the electronic and ionic contributions of the total electrical conductivity, the first temperature-dependent measurement between 450 and 900 °C was carried out in air giving the ionic conductivity of the materials. All measurements in reducing atmosphere were carried out in flowing Ar/4% H_2 atmosphere. Under these conditions, the partial pressure of oxygen at 900 °C varied between 1.3 and 2.9×10^{-21} bar due to the presence of moisture (200–300 ppm). The same procedure was used for the measurements of the total electrical conductivity of the Ni/YZT cermets in Ar/4% H_2. The cermet samples, on which the electrical properties were determined, were cut before and after exposure at 1,000 °C for 1,000 h and the microstructure of their cross-sectional surfaces was investigated by optical microscopy and digital image analysis.

For the electrochemical test, 40 vol% Ni/8YSZ anode substrates with porosity of about 40% and dimensions 50 × 50 × 1.5 mm, sintered at 1,400 °C for 3 h in air, were used. The substrates were coated by vacuum slip casting using diluted suspensions of NiO and YZT ceramic for the fabrication of anode functional layers with 40 vol% Ni after reduction [24]. The subsequent deposition of electrolyte and cathode layers (active surface area 40 × 40 mm) was carried out using vacuum slip casting and screen printing, respectively. Cell manufacturing and

electrochemical testing were performed as described elsewhere [25].

Results and discussion

Crystal structure characterisation

The crystalline phases formed after sintering at 1,400 °C for 5 h are listed in Table 1. All powders are cubically crystallised except the sample no. 6 with Ti content of 10 at%, which shows minor peaks of the tetragonal structure besides the cubic reflections [17]. In the same sample TiO_2 is not completely dissolved in the zirconia matrix at lower temperatures and small reflections of the rutile-type structure appear in the diffractograms. Full dissolution of titania occurred at 1,400 °C.

In powder no. 4 additional reflections started to appear at about 1,200 °C attributed to the formation of a pyrochlore-type structure [$Y_2(Ti,Zr)_2O_7$], which decomposed with increasing temperature and disappeared at 1,500 °C [22]. These results are in good agreement with the experimentally established [20, 21] or theoretically predicted [26] phase diagram (Fig. 1).

Electrical conductivity of ceramics

Figure 2 shows the Arrhenius plots of the effective electrical conductivity (σ_{ef}) of the investigated ceramics in the temperature range of 450–900 °C, according to the formula for ionic conductivity:

$$\sigma_{ef}T = k\exp(-E_a/RT) \quad (1)$$

where E_a = activation energy, k = pre-exponential factor, R = gas constant, T = absolute temperature.

Several general features can be deduced from the conductivity in air and in Ar/4% H_2 atmosphere.

- In air (Fig. 2a):

The conductivity decreases with increasing Ti content (by about one order of magnitude at 900 °C) and becomes almost independent of Y content. For the same Y content, the activation energy remains practically constant with Ti content. This behaviour can be attributed to the fact that some of the mobile oxygen vacancies are trapped by the Ti cations and therefore fewer sites are available for ion hopping [8] without any significant influence on the charge carrier mobility [27]. At the same Ti level (5 at%) the conductivity passes through a maximum for Y content

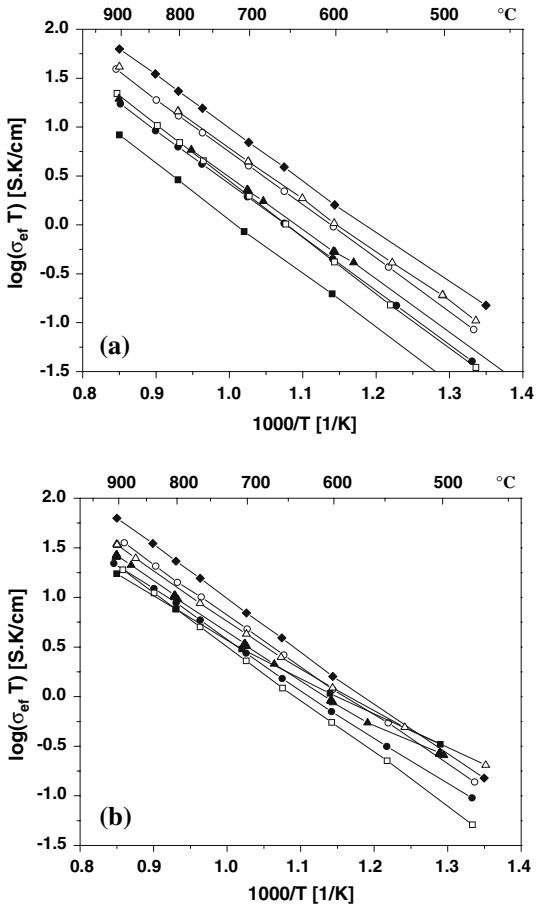

Fig. 2 Total effective electrical conductivity of $Y_{0.20}Zr_{0.75}Ti_{0.05}O_{1.9}$ (○), $Y_{0.20}Zr_{0.70}Ti_{0.10}O_{1.9}$ (●), $Y_{0.25}Zr_{0.70}Ti_{0.05}O_{1.875}$ (□), $Y_{0.25}Zr_{0.60}Ti_{0.15}O_{1.875}$ (■), $Y_{0.141}Zr_{0.809}Ti_{0.05}O_{1.930}$ (Δ), $Y_{0.133}Zr_{0.767}Ti_{0.10}O_{1.934}$ (▲) and $Y_{0.148}Zr_{0.852}O_{1.926}$ (8YSZ) (◆) ceramics, measured (**a**) in air and (**b**) in Ar/4% H_2

Table 1 Nominal powder compositions, crystalline phases (c, cubic; t, tetragonal; p, pyrochlore) and lattice parameters (α_c) of the cubic phase after sintering at 1,400 °C

No.	Nominal composition	Detected phases	Lattice parameter a_c of the cubic phase (pm)
1	$Y_{0.20}Zr_{0.75}Ti_{0.05}O_{1.9}$	c	513.1(8)
2	$Y_{0.20}Zr_{0.70}Ti_{0.10}O_{1.9}$	c	512.0(9)
3	$Y_{0.25}Zr_{0.70}Ti_{0.05}O_{1.875}$	c	513.6(4)
4	$Y_{0.25}Zr_{0.60}Ti_{0.15}O_{1.875}$	c + (p)	512.5(2)
5	$Y_{0.141}Zr_{0.809}Ti_{0.05}O_{1.930}$	c	513.0(3)
6	$Y_{0.133}Zr_{0.767}Ti_{0.10}O_{1.934}$	c + (t)	512.7(1)
7	$Y_{0.148}Zr_{0.852}O_{1.926}$ (8YSZ)	c	513.9(4)

between 14.1 and 25 at%, whereas the activation energy increases continuously. This is due to opposing mechanisms, as has been reported for the Y–Zr–O system [28, 29]. On the one hand, for low Y contents (<14 at%) the dominant factor is the increasing number of point defects (oxygen vacancies) resulting in increasing conductivity, while the activation energy does not change significantly. On the other hand, for high Y contents (>20 at%) the dominant factor is the interaction between defects resulting in decreasing conductivity and increasing activation energy. In all cases, the conductivity values of the ceramic materials of the quasi-ternary system are below the corresponding values for 8YSZ.

- In Ar/4% H_2 (Fig. 2b):

The results show that the absolute conductivity values of the Y–Zr–Ti–O ceramics in Ar/4% H_2 (Fig. 2b) are higher than those in air (Fig. 2a), but below the corresponding values of 8YSZ at high temperatures. The differences between the conductivity values in Ar/4% H_2 compared to the values in air increase with increasing Ti content. There is a stronger increase in conductivity at low temperatures and high Ti content due to the electron hopping mechanism between the Ti^{4+} and Ti^{3+} oxidation states of titanium, which leads to an additional electronic n-type conductivity. Furthermore, the activation energy decreases with increasing Ti content indicating mixed ionic-electronic character. From the above analysis, it is obvious that the electronic conductivity of the YZT ceramics is too low to replace the metallic Ni in the "state-of-the-art" Ni/8YSZ cermet anode of an SOFC.

After the conductivity measurements the porosity (P) of the rectangular bars was used to correct the measured effective conductivity (σ_{ef}) of the ceramics and to calculate their specific conductivity (σ_0). According to the measured data for oxides given by Mizusaki et al. [30] the plot of the ratio σ_{ef}/σ_0 vs. P follows a straight line for small porosities and σ_{ef}/σ_0 converges to 0 at $P = 0.4$–0.55. In this case and for porosity less than 0.25 the relationship given for isotropic materials with randomly oriented ellipsoids as porous phase [31] is

$$\sigma_{ef} = \sigma_0(1 - m\,P) \qquad (2)$$

and fairly well reproduces the σ_{ef}/σ_0 vs. P dependence with the empirically determined parameter of $m = 2.1$.

Table 2 includes the porosity, the specific electrical conductivity values, Eq. (2), at 900 °C in air and Ar/4% H_2, as well as the corresponding activation energies, Eq. (1). The validity of Eq. (2) for the calculation of the specific conductivity was checked in comparison to literature data obtained at 900 °C in air for similar compounds. The value of 61.3 mS/cm for 8YSZ (Table 2) is in the range 57.4–90 mS/cm reported for 8 or 9 mol%YSZ [32, 33]. The values 41.5 and 20.8 mS/cm obtained for samples 1 and 2 with 5 and 10 mol% TiO_2 additions agree well with the reported values [2] of 38.4 and 12.6 mS/cm, respectively. In all cases the reported values are referred to highly dense samples (99% of theoretical density).

Electrical conductivity and microstructure stability of Ni/YZT cermets

The temperature dependence of the electrical conductivity of Ni/YZT cermets with 30, 40 and 45 vol% Ni shows that all the specimens exhibited metallic character, whereas the absolute values depended on the Ni content. Samples with 30 vol% Ni were at the percolation limit of the S-shaped curve of electrical conductivity for cermets with 20–25% porosity [15] and therefore possessed much lower conductivity values.

The long-term stability of the electrical conductivity of Ni/YZT cermets was examined after exposure at 1,000 °C in Ar/4% H_2 atmosphere up to 1,000 h. At fixed time intervals the annealing was interrupted and the electrical conductivity of the samples was measured in the temperature range of 25–900 °C. Figure 3 illustrates the time-dependent electrical conductivity of the Ni/YZT cermets containing 30, 40 and 45 vol% Ni (Fig. 3a–c, respectively), measured at 900 °C. The initial scatter at $t = 0$ h of the electrical conductivity values among the samples with same Ni content is mainly attributed to the difference in the porosity reflecting the final stage of sample preparation.

A significant factor for the evaluation of the stability of the cermets after long-term annealing is the difference between the initial ($t = 0$ h) and the time dependent (up to 1,000 h) electrical conductivity values. Among all the investigated systems $Ni/Y_{0.148}Zr_{0.852}O_{1.926}$ (Ni/8YSZ) showed the highest decrease in conductivity, reaching the lowest values after 1,000 h of exposure, independent of Ni content (Fig. 3). Regarding the electrical conductivity of the 30 vol% Ni/8YSZ cermet (Fig. 3a), the values decreased significantly after the first 300 h of exposure exhibiting an ionic-type conduction mechanism [15]. In the Ni/YZT cermets the difference between the initial and final conductivity values decreased with increasing Ni and TiO_2 content reaching steady-state values within the first 500 h of exposure. For Ni/YZT cermets with the same Ni and TiO_2 content, an increase of Y_2O_3 content followed in general an increase in loss of conductivity with exposure time (Fig. 3).

Post-examination on metallographic cross-sections of the cermet samples on which the electrical properties were determined, was performed by optical microscopy and digital image analysis. Table 3 lists the results concerning the mean diameter $(\overline{d}_{Ni})$ of the Ni particles before ($t = 0$ h)

Table 2 Specific electrical conductivity ($\sigma_{0,\ 900\ °C}$) of YZT ceramics measured in air and Ar/4%H_2 and the corresponding activation energies (E_a) between 450 and 900 °C

Sample	Nominal composition	Porosity,	Measurement in air		Measurement in Ar/4%H_2	
No.	$Y_xZr_{1-x-y}Ti_yO_{2-x/2}$	P (%)	$\sigma_{0,\ 900\ °C}$ (mS cm^{-1})	E_a (eV)	$\sigma_{0,\ 900\ °C}$ (mS cm^{-1})	E_a (eV)
1	$Y_{0.20}Zr_{0.75}Ti_{0.05}O_{1.9}$	13	41.5	1.08	44.8	1.00
2	$Y_{0.20}Zr_{0.70}Ti_{0.10}O_{1.9}$	14	20.8	1.09	26.4	0.98
3	$Y_{0.25}Zr_{0.70}Ti_{0.05}O_{1.875}$	17	26.2	1.14	27.3	1.07
4	$Y_{0.25}Zr_{0.60}Ti_{0.15}O_{1.875}$	5	7.9	1.12	16.5	0.77
5	$Y_{0.141}Zr_{0.809}Ti_{0.05}O_{1.930}$	6	37.0	1.05	33.0	0.92
6	$Y_{0.133}Zr_{0.767}Ti_{0.10}O_{1.934}$	5	18.5	1.06	25.8	0.91
7	$Y_{0.148}Zr_{0.852}O_{1.926}$ (8YSZ)	6	61.3	1.05	61.3	1.05

and after (t = 1,000 h) exposure at 1,000 °C in reducing atmosphere for the Ni/YZT and Ni/8YSZ [17] cermets with 30 and 40 vol% Ni. The extent of agglomeration and grain coarsening of Ni particles influences the long-term stability of the cermets, interrupting the metal network continuity (Ni–Ni contacts) and therefore reducing the conduction pathways in the cermets.

For the 30 vol% Ni/8YSZ cermet material with porosity of about 20%, the increase of the mean Ni diameter by about 15% is in good agreement with the value 13.2% for the 40 vol% Ni/8YSZ cermet with 40% porosity given by Simwonis et al. [34]. Regarding the 30 vol% Ni/YZT cermets the coarsening of Ni particles leads to an increase of the mean diameter between 5 and 15%, depending on Y_2O_3 and TiO_2 contents in the ceramic phase. For the same Y_2O_3 content, increasing presence of TiO_2 suppresses the agglomeration rate of Ni particles, whereas the increasing presence of Y_2O_3 acts in the opposite way (Table 3). In the case of 30 vol% Ni cermets, the metal content is close to the percolation limit of the S-shaped curve of the electrical conductivity and consequently small changes in the mean diameter ($\bar{d}_{Ni}$), cause significant differences in their values before and after annealing (Fig. 3a).

For the 40 vol% Ni/YZT cermets the presence of TiO_2 in the ceramic phase leads to an increase of the mean diameter ($\bar{d}_{Ni}$) in the range of 10–20% compared to 99% for the 40 vol% Ni/8YSZ cermet (Table 3), enhancing in this way the long-term stability of the electrical conductivity of the cermets (Fig. 3b). A more pronounced trend is observed for the cermets with high metal content (45 vol% Ni), in which the Ni metal acts as matrix phase.

Micrographs (Fig. 4) of the 40 vol% Ni/$Y_{0.20}Zr_{0.70}Ti_{0.10}O_{1.9}$ cermet before (Fig. 4a) and after (Fig. 4b) annealing at 1,000 °C for 1,000 h in reducing atmosphere verify the electrical conductivity results, showing the reduced tendency of agglomeration and grain coarsening of the Ni particles in these cermets in comparison to 40 vol% Ni/8YSZ cermets [17].

The positive influence of TiO_2 presence on the structural stability of cermets can be explained in terms of interfacial properties. According to wettability results [18] additions of the low-surface energy TiO_2 in the ceramic matrix improve the interfacial bonding between solid Ni and the ceramic phase. The enhanced adherence at the metal/ceramic interface restrains the movement of the Ni particles on the plane of contact with the ceramic. The resulting smaller vibration modes at the particle interface suppressing its agglomeration tendency maintain a continuous metallic network throughout the Ni/YZT cermets. The sustained electrical conductivity values (Fig. 3), attributed to the increased structure stability of the cermet, improve the long-term stability of the SOFC anodes even if the amount of metal is close to the percolation limit of the matrix.

In the case of Ni/$Y_{0.25}Zr_{0.60}Ti_{0.15}O_{1.875}$ cermets with 40 and 45 vol% Ni and high TiO_2 content (Fig. 3b, c), the increase in adhesion energy (work of adhesion) at the metal/ceramic interface promotes the broadening of the metal at the ceramic surface during the initial stages of annealing. Hence, the spreading of the Ni particles positively influence the establishment of an improved continuous metallic network through the cermet microstructure causing higher conductivity values. This process is superimposed by the partial sintering of the Ni particles leading to limited coarsening at the steady state and inducing slight decrease in conductivity [15].

Electrochemical tests

The possible use of Ni/YZT cermets as anode materials was evaluated in terms of its application in an SOFC. For this purpose three cermets with increasing Ti content were selected: the "state-of-the-art" Ni/8YSZ, Ni/$Y_{0.20}Zr_{0.75}Ti_{0.05}O_{1.9}$ and Ni/$Y_{0.20}Zr_{0.70}Ti_{0.10}O_{1.9}$. For the fuel cells with these anode functional layers, the anode

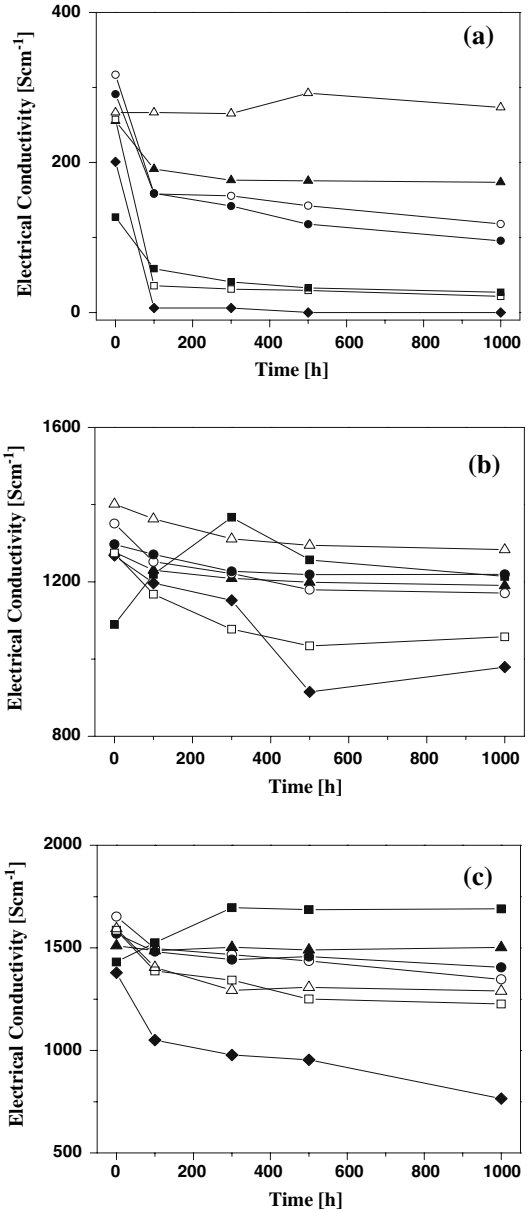

Fig. 3 The variation of electrical conductivity at 900 °C as a function of annealing time at 1,000 °C in Ar/4% H_2 for (**a**) 30, (**b**) 40 and (**c**) 45 vol% Ni-cermets with ceramic phases: $Y_{0.20}Zr_{0.75}Ti_{0.05}O_{1.9}$ (○), $Y_{0.20}Zr_{0.70}Ti_{0.10}O_{1.9}$ (●), $Y_{0.25}Zr_{0.70}Ti_{0.05}O_{1.875}$ (□), $Y_{0.25}Zr_{0.60}Ti_{0.15}O_{1.875}$ (■), $Y_{0.141}Zr_{0.809}Ti_{0.05}O_{1.930}$ (Δ), $Y_{0.133}Zr_{0.767}Ti_{0.10}O_{1.934}$ (▲) and $Y_{0.148}Zr_{0.852}O_{1.926}$ (8YSZ) (◆)

substrate, electrolyte and cathode were fabricated in the same batch to guarantee a reliable comparison of the cell test results. The current-voltage curves at 800 °C in H_2/3% H_2O and in 33% CH_4/67% H_2O are illustrated in Fig. 5. In comparison to the formerly reported results [15] the performance of the cells were strongly improved which is mainly the reason of cathode optimization [25, 35]. Therefore the cells with Ni/8YSZ serve as a reference for the cells with Ti-containing anode cermets.

In H_2/3% H_2O the current–voltage curves are very close together for the three different anode materials and only the cell with the Ni/$Y_{0.20}Zr_{0.75}Ti_{0.05}O_{1.9}$ anode showed a cell voltage that is 30 mV higher than the two other cells. Under steam reforming conditions with CH_4/H_2O = 1:2 the cells with Ni/8YSZ and Ni/$Y_{0.20}Zr_{0.75}Ti_{0.05}O_{1.9}$ anode showed a comparable performance, with a larger scatter of the U–i curves as indicated by the error bars indicating the results of two measured cells for each anode composition. The cell containing the anode functional layer with the highest amount of titania, Ni/$Y_{0.20}Zr_{0.70}Ti_{0.10}O_{1.9}$, revealed a reduction in cell performance lower than the two other cells by 40–50 mV. This tendency confirms earlier results indicating that even higher Ti contents lead to decreasing cell performances [15]. In summary, the mixed-conductivity of YZT ceramics slightly promotes the fuel gas conversion as long as the Ti content is up to around 5 at% and H_2 is used as fuel. For higher Ti concentrations the performance of SOFCs decreases compared to conventional anode cermets. From the here presented results it can be concluded that the decreasing ionic conductivity is overcompensating the small beneficial effect of the increasing mixed conductivity (Fig. 2).

Conclusions

YZT ceramics with composition $Y_xZr_{1-x-y}Ti_yO_{2-x/2}$ were synthesised and investigated with respect to their crystal structure, electrical conductivity and long-term stability of the corresponding Ni/YZT cermets containing 30, 40 and 45 vol% Ni. The partial substitution of ZrO_2 by TiO_2 in the fluorite structure, especially for high titania and yttria contents, leads to the formation of a second phase with pyrochlore type structure, which decomposes after calcinations at high temperatures (1,500 °C). The electrical conductivity of the YZT ceramics with high TiO_2 content showed a significant contribution of electronic conductivity in reducing atmosphere but a decreased ionic conductivity in air.

The Ni/YZT cermets showed an improved structural stability after annealing at 1,000 °C for 1,000 h in Ar/4%H_2 due to the enhanced bond strength at the metal/ceramic interface, which causes the reduction of agglomeration rate of Ni particles. The improved structural stability of cermets suppresses the loss of electrical conductivity after annealing.

The electrochemical tests on fuel cells with Ni/8YSZ and Ni/$Y_{0.20}Zr_{0.75}Ti_{0.05}O_{1.9}$ anodes showed comparable

Table 3 Mean grain size of the Ni particles ($\bar{d}_{Ni}$) for the cermets containing 30 and 40 vol% Ni before and after annealing at 1,000 °C for 1,000 h in Ar/4% H_2 atmosphere

No.	Cermet	Ni (vol%)	$\bar{d}_{Ni,\ 0\ h}$ (μm)	$\bar{d}_{Ni,\ 1{,}000\ h}$ (μm)	$\bar{d}_{Ni}$ increase (%)
1	$Ni/Y_{0.20}Zr_{0.75}Ti_{0.05}O_{1.9}$	30	1.55	1.75	12.9
		40	1.57	1.81	15.3
2	$Ni/Y_{0.20}Zr_{0.70}Ti_{0.10}O_{1.9}$	30	1.55	1.68	8.4
		40	1.71	1.88	9.9
3	$Ni/Y_{0.25}Zr_{0.70}Ti_{0.05}O_{1.875}$	30	1.59	1.83	15.1
		40	1.68	1.99	18.5
4	$Ni/Y_{0.25}Zr_{0.60}Ti_{0.15}O_{1.875}$	30	1.11	1.25	12.6
		40	1.17	1.36	16.2
5	$Ni/Y_{0.141}Zr_{0.809}Ti_{0.05}O_{1.930}$	30	1.46	1.53	4.8
		40	1.65	1.98	20.0
6	$Ni/Y_{0.133}Zr_{0.767}Ti_{0.10}O_{1.934}$	30	1.48	1.58	6.8
		40	1.62	1.83	13.0
7	$Ni/Y_{0.148}Zr_{0.852}O_{1.926}$ (Ni/8YSZ)	30	1.44	1.66	15.3
		40	1.56	3.11	99.4

* Values for samples 4 and 7 from Ref. [15]

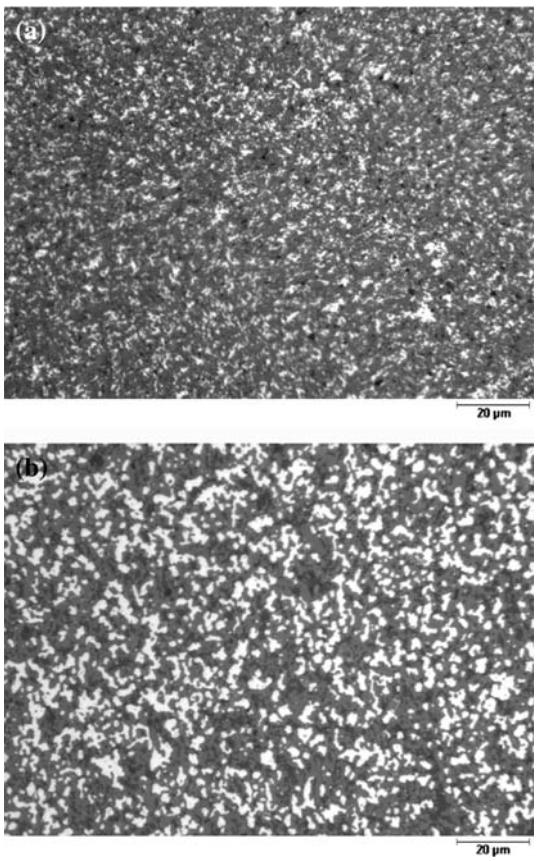

Fig. 4 Micrographs of the 40 vol% $Ni/Y_{0.20}Zr_{0.70}Ti_{0.10}O_{1.9}$ cermet before (**a**) and after annealing (**b**) at 1,000 °C for 1,000 h in Ar/4% H_2 atmosphere. The scale bar corresponds to 20 μm. White: Ni, grey: YZT, black: pores

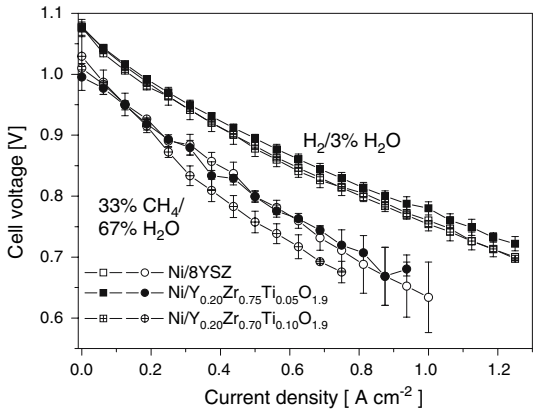

Fig. 5 U–i curves at 800 °C using H_2/3%H_2O (squares) and 33% CH_4/67% H_2O (circles) as fuel gas for fuel cells with 40 vol% Ni/8YSZ (open symbols), 40 vol% $Ni/Y_{0.20}Zr_{0.75}Ti_{0.05}O_{1.9}$ (filled symbols) and 40 vol% $Ni/Y_{0.20}Zr_{0.70}Ti_{0.10}O_{1.9}$ (crossed symbols) anodes

performance at 800 °C using H_2/3% H_2O and 33% CH_4/67% H_2O as fuel gas. However, the improved structural stability of the $Ni/Y_{0.20}Zr_{0.75}Ti_{0.05}O_{1.9}$ anode is expected to reveal a superior long-term performance compared to Ni/8YSZ, especially at higher working temperatures.

For YZT ceramics with higher Ti content, as in the case of Ni/ $Y_{0.20}Zr_{0.70}Ti_{0.10}O_{1.9}$, the significant lowering of the ionic conductivity, compared to 8YSZ, reduces the flux of oxygen ions towards the three-phase boundaries in the Ni/YZT anode, which is a limiting factor for the electrochemical conversion of the fuel.

Acknowledgements Financial support is gratefully acknowledged from the Greek-German (GRC 01/099) bilateral co-operation project and from the E.U. Integrated Project REALSOFC (No. SES6-CT-2003–50261). The authors thank the colleagues at IEF—S. Heinz, V. Bader, G. Blaß, W. Herzhof, C. Tropartz—for technical assistance and M. Michulitz (FZJ-ZCH) for chemical analysis with ICP-OES.

References

1. Liou SS, Worrell WL (1989) Appl Phys A 49:25
2. Naito H, Arashi H (1992) Solid State Ionics 53–56:436
3. Colomer MT, Traqueia LSM, Jurado JR, Marques FMB (1995) Mater Res Bull 30:515
4. Rog G, Borchardt G (1996) Ceram Int 22:149
5. Swider KE, Worrell WL (1996) J Electrochem Soc 143:3706
6. Traqueia LSM, Pagnier T, Marques FMB (1997) J Eur Ceram Soc 17:1019
7. Kobayashi K, Kai Y, Yamaguchi S, Fukatsu N, Kawashima T, Iguchi Y (1997) Solid State Ionics 93:193
8. Kaiser A, Feighery AJ, Fagg DP, Irvine JTS (1998) Ionics 4:215
9. Capel F, Moure C, Duran P, Gonzalez-Elipe AR, Caballero A (2000) J Mater Sci 35:345
10. Hui S, Petric A (2002) J Eur Ceram Soc 22:1673
11. Pudmich G, Boukamp BA, Gonzalez-Cuenca M, Jungen W, Zipprich W, Tietz F (2000) Solid State Ionics 135:433
12. Primdahl S, Mogensen M (2002) Solid State Ionics 152–153:597
13. Skarmoutsos D, Tsoga A, Naoumidis A, Nikolopoulos P (2000) Solid State Ionics 135:439
14. Ruiz-Morales JC, Nunez P, Buchanan R, Irvine JTS (2003) J Electrochem Soc 150:A1030
15. Skarmoutsos D, Nikolopoulos P, Tietz F, Vinke IC (2004) Solid State Ionics 170:153
16. Laguna-Bercero MA, Larrea A, Peña JI, Merino RI, Orera VM (2005) J Eur Ceram Soc 25:1455
17. Skarmoutsos D, Tietz F, Nikolopoulos P (2001) Fuel Cells 1:243
18. Mantzouris X, Zouvelou N, Skarmoutsos D, Nikolopoulos P, Tietz F (2005) J Mater Sci 40:2471
19. Tsoga A, Naoumidis A, Nikolopoulos P (1996) Acta Mater 44:3679
20. Colomer MT, Duran P, Caballero A, Jurado JR (1997) Mat Sci Eng A 229:114
21. Feighery AJ, Irvine JTS, Fagg DP, Kaiser A (1999) J Solid State Chem 143:273
22. Tietz F, Jungen W, Lersch P, Figaj H, Becker KD, Skarmoutsos D (2002) Chem Mater 14:2252
23. Kountouros P, Förthmann R, Naoumidis A, Stochniol G, Syskakis E (1995) Ionics 1:40
24. Buchkremer HP, Diekmann U, Stöver D (1996) In: Thorstensen B (ed) Proceedings of 2nd Eur. SOFC Forum, Oslo, The European Fuel Cell Forum, Oberrohrdorf, Switzerland, p 221
25. Mertens J, Haanappel VAC, Tropartz C, Herzhof W, Buchkremer HP (2006) J Fuel Cell Sci Technol 3:125
26. Yokokawa H, Sakai N, Kawada T, Dokiya M (1993) In: Badwal SPS, Bannister MJ, Hannink RHJ (eds) Proceedings of Science and Technology of Zirconia V, Technomic Publ. Co., Lancaster, Pennsylvania, USA, p 59
27. Tietz F, Arul Raj I., Stöver D (2004) Brit Ceram Trans 103:202
28. Ioffe AI, Rutman DS, Karpachov SV (1978) Electrochim Acta 23:141
29. Schmalzried H (1977) Z Phys Chem Neue Folge 105:47
30. Mizusaki J, Warangai K, Tsuchiya S, Tagawa H, Arai Y, Kuwayama Y (1996) J Am Ceram Soc 79:109
31. McLachlan DS, Blaszkiewicz M, Newnham RE (1990) J Am Ceram Soc 73:2187
32. Van Herle J, McEvoy AJ, Ravindranathan Thampi K (1994) J Mater Sci 29:3691
33. Ciacchi FT, Crane KM, Badwal SPS (1994) Solid State Ionics 73:49
34. Simwonis D, Tietz F, Stöver D (2000) Solid State Ionics 132:241
35. Haanappel VAC, Mertens J, Rutenbeck D, Tropartz C, Herzhof W, Sebold D, Tietz F (2005) J Power Sources 141:216